Breakdown of single spin-fluid model in the heavily hole-doped superconductor $CsFe_2As_2$

D. Zhao,[1] S. J. Li,[1] N. Z. Wang,[1] J. Li,[1] D. W. Song,[1] L. X. Zheng,[1] L. P. Nie,[1] X. G. Luo,[1,2,3] T. Wu,[1,2,3,*] and X. H. Chen[1,2,3]

[1]*Hefei National Laboratory for Physical Science at Microscale and Department of Physics, University of Science and Technology of China, Hefei, Anhui 230026, China*

[2]*Key Laboratory of Strongly-coupled Quantum Matter Physics, University of Science and Technology of China, Chinese Academy of Sciences, Hefei 230026, China*

[3]*Collaborative Innovation Center of Advanced Microstructures, Nanjing University, Nanjing 210093, China*

(Received 27 May 2017; revised manuscript received 9 November 2017; published 16 January 2018)

Although Fe-based superconductors are correlated electronic systems with multiorbital, previous nuclear magnetic resonance (NMR) measurement suggests that a single spin-fluid model is sufficient to describe its spin behavior. Here, we first observed the breakdown of single spin-fluid model in a heavily hole-doped Fe-based superconductor $CsFe_2As_2$ by site-selective NMR measurement. At high-temperature regime, both Knight shift and nuclear spin-lattice relaxation at ^{133}Cs and ^{75}As nuclei exhibit distinct temperature-dependent behavior, suggesting the breakdown of the single spin-fluid model in $CsFe_2As_2$. This is ascribed to the coexistence of both localized and itinerant spin degree of freedom at 3*d* orbitals, which is consistent with the orbital-selective Mott phase. With decreasing temperature, the single spin-fluid behavior is recovered below $T^* \sim 75$ K due to a coherent state among 3*d* orbitals. The Kondo liquid scenario is proposed to understand the low-temperature coherent state.

DOI: 10.1103/PhysRevB.97.045118

I. INTRODUCTION

In high-T_c cuprate superconductors, the single spin-fluid model has been widely adopted as a theoretical starting point although at least one 3*d* and two 2*p* orbitals from copper and oxygen sites should be considered together in the theoretical model in principle [1]. Such hypothesis is mostly based on the celebrated concept of the Zhang-Rice singlet [2], which successfully converts the complex reality into a single-band *t*-*J* model. Such a single spin-fluid model has been validated by early site-selective nuclear magnetic resonance (NMR) measurement on ^{89}Y, ^{63}Cu, and ^{17}O nuclei in $YBa_2Cu_3O_{6+x}$ [3,4].

In Fe-based superconductors, the multiorbital nature is a key factor to understand its basic properties [5]. Considering the correlation effect due to Hund's coupling, the single spin-fluid model should be insufficient in this case [6,7]. However, previous site-selective NMR measurement on F-doped LaOFeAs found that Knight shift and nuclear spin-lattice relaxation on different nuclei are nearly identical [8], including ^{75}As, ^{57}Fe, ^{19}F, and ^{139}La nuclei. This result supports a single spin-fluid scenario in the frame of weak coupling theory based on the itinerant nature of Fe 3*d* electrons [9,10]. Similar behavior was also observed in many other Fe-based superconductors [11–13]. On the other hand, the strong coupling theory based on the local nature of Fe 3*d* electrons has also been proposed for Fe-based superconductors [14], in which the coexistence of itinerant and localized electrons at different 3*d* orbitals would appear in a so-called orbital-selective Mott phase [15–17]. Recently, the orbital-selective Mott phase has been widely observed in FeSe-derived superconductors by angle-resolved photoemission spectroscopy (ARPES) [18,19]. However, the site-selective NMR experiment has not yet observed breakdown of the single spin-fluid model in these FeSe-derived superconductors [11].

Very recently, a similar orbital-selective Mott phase has been suggested in the heavily hole-doped Fe-based superconductors AFe_2As_2 (A = K, Rb, Cs) [20,21]. A so-called Knight shift anomaly phenomenon has been observed by the previous ^{75}As NMR in AFe_2As_2 (A = K, Rb, Cs) [22], which hints at a possible coexistence of local and itinerant 3*d* electrons. However, how to distinguish the origin of the local moment among five 3*d* orbitals needs a orbital-selective probe, which is also a direct checkout for the single spin-fluid model. Here, we first achieve a orbital-selective measurement of $CsFe_2As_2$ single crystal by a site-selective NMR measurement on ^{133}Cs and ^{75}As nuclei. Our results strongly support the breakdown of the single-fluid model, and reveal the key role of $3d_{xy}$ orbital on the origin of the local moment.

For a multiorbital system, the spin part of Knight shift due to different 3*d* orbitals can be simply written as the following expression:

$$K_s(T) = \sum_{\sigma} A_\sigma \chi_\sigma(T), (\sigma = xz, yz, xy, z^2, x^2 + y^2). \quad (1)$$

A_σ is the hyperfine coupling tensor from different 3*d* orbitals. $\chi_\sigma(T)$ is the orbital-dependent local spin susceptibility. In the paramagnetic state, the Knight shift of both ^{133}Cs and ^{75}As nuclei is dominated by transferred hyperfine interaction through the overlap with the 4*s*/6*s* orbital (see Supplemental Material [23] for details and Ref. [12]) as shown in Fig. 1(a). Considering the difference on spatial distribution along the *c* axis among the five 3*d* orbitals at Fe sites, the hyperfine coupling tensors for $3d_{xy}$ and $3d_{x^2+y^2}$ orbitals are almost negligible for ^{133}Cs nuclei due to the less overlap with 6*s* orbital. Therefore, the Knight shift of ^{133}Cs nuclei is only

*wutao@ustc.edu.cn

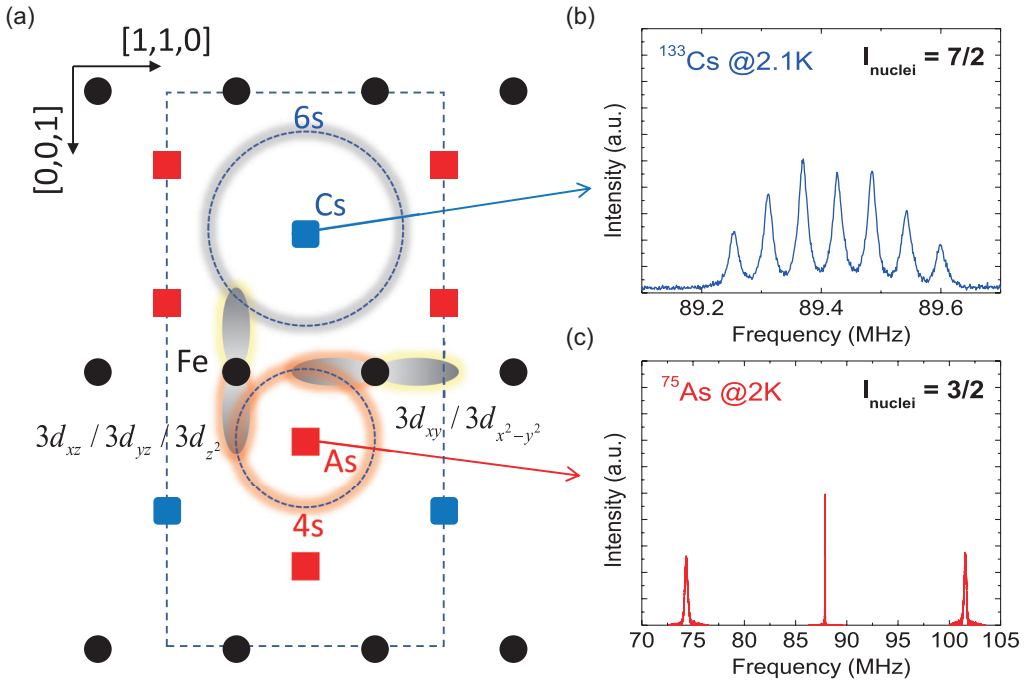

FIG. 1. (a) Illustration of the microscopic process of the dominated contribution on Knight shift due to transferred hyperfine interaction at ^{75}As and ^{133}Cs sites. The crystalline structure of $CsFe_2As_2$ is shown in the side view along Fe-Fe direction. The hyperfine interaction contributed to Knight shift of ^{75}As and ^{133}Cs are dominated by the transferred hyperfine interaction through the hybridization of on-site 4*s* or 6*s* orbital with 3*d* orbitals at the nearest-neighbor Fe atoms. We performed NMR measurements on both ^{75}As and ^{133}Cs nuclei. The full spectrum at 2 K are shown in (b) for ^{133}Cs nuclei and (c) for ^{75}As nuclei.

sensitive to local spin susceptibility due to $3d_{xz}$, $3d_{yz}$, and $3d_{z^2}$ orbitals. In contrast, all five 3*d* orbitals contribute to the Knight shift of ^{75}As nuclei. By comparing the temperature-dependent Knight shift of both ^{133}Cs and ^{75}As nuclei, we can qualitatively extract useful information on orbital-dependent spin susceptibility, suggesting an orbital-selective NMR probe. Based on the above analysis, the site-selective NMR by measuring both ^{75}As and ^{133}Cs nuclei has the ability to examine the single spin-fluid model. The following results unambiguously confirm the breakdown of the single spin-fluid model in heavily hole-doped Fe-based superconductor $CsFe_2As_2$.

II. EXPERIMENTAL METHOD

High-quality $CsFe_2As_2$ single crystals are grown by the self-flux technique [24]. All NMR measurement on ^{75}As and ^{133}Cs nuclei are conducted from 2–300 K under an external magnetic field of 16 Tesla parallel to the *c* axis. The nuclear spin number I_{nuclei} for ^{75}As and ^{133}Cs nuclei are 3/2 and 7/2, respectively. The standard full spectrum of ^{75}As and ^{133}Cs nuclei are shown in Figs. 1(b) and 1(c). There are three transition lines for ^{75}As nuclei and seven transition lines for ^{133}Cs nuclei. For ^{133}Cs nuclei, all transition lines have a similar linewidth of ∼20 kHz at 2 K, suggesting a magnetic dominated broadening effect. For ^{75}As nuclei, the linewidth for satellites and central line at 2 K are quite different with the values of ∼300 kHz and ∼30 kHz, respectively. This is due to a quadrupole dominated broadening effect on satellites. Similar behavior has been seen in a previous study [25]. By measuring the separation between each transition lines, the quadrupole frequency υ_Q for ^{75}As and ^{133}Cs nuclei are determined to be ∼13.6 MHz and ∼0.058 MHz, respectively. Both Knight shifts for ^{75}As and ^{133}Cs nuclei are determined by measuring the peak position on central transition line. Nuclear spin-lattice relaxations rates $1/T_1$ are measured on the central transition line for both ^{75}As and ^{133}Cs nuclei.

III. EXPERIMENTAL RESULTS

The main results in this work are shown in Fig. 2. As shown in Fig. 2(a), the temperature-dependent Knight shift of ^{75}As (^{75}K) nuclei exhibits a characteristic crossover behavior. At high-temperature regime, ^{75}K is gradually increasing with decreasing temperature. This is consistent with the high-temperature bulk magnetic susceptibility, suggesting a localized spin behavior [22]. With further decreasing temperature, ^{75}K shows a maximum and then starts to decrease with lowering temperature. Below 20 K, ^{75}K becomes saturated and shows a temperature-independent behavior. The temperature-dependent behavior is ascribed to an incoherent-to-coherent electronic crossover, which is also observed in KFe_2As_2 and $RbFe_2As_2$ with different crossover temperatures [22]. In sharp contrast, the remarkable crossover behavior in temperature-dependent Knight shift of ^{75}As nuclei is completely absent in that of ^{133}Cs nuclei. As shown in Fig. 2(a), the localized spin behavior is absent in the temperature-dependent Knight shift of ^{133}Cs (^{133}K) nuclei, which shows a monotonous decrease down to 2 K. As we discussed before, in contrast to ^{75}K, the ^{133}K is only sensitive to $3d_{xz}$, $3d_{yz}$, and $3d_{z^2}$ orbitals. If the local spin behavior in the temperature-dependent ^{75}K only comes from

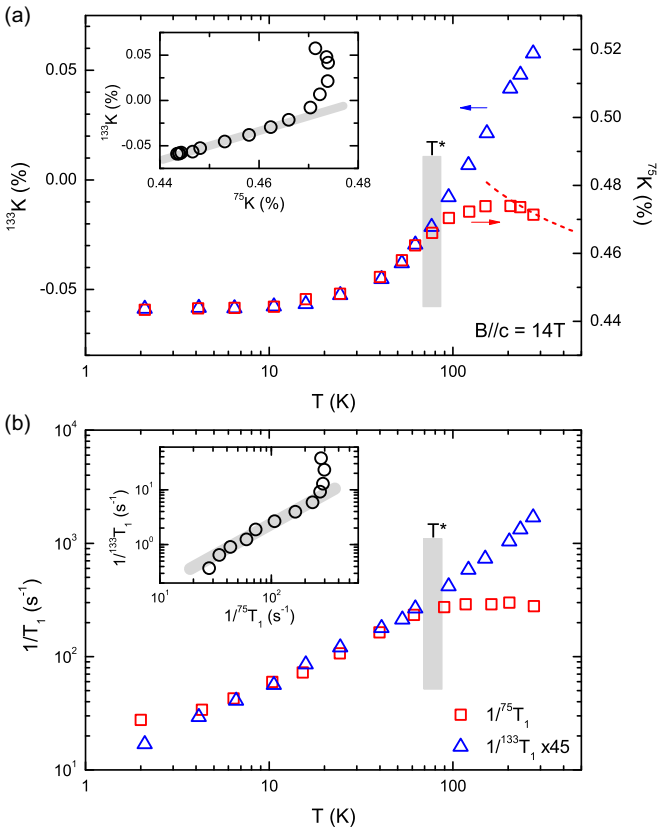

FIG. 2. (a) Temperature-dependent Knight shift for both ^{75}As and ^{133}Cs nuclei. The blue triangles represent the Knight shift of ^{133}Cs nuclei. The red squares represents the Knight shift of ^{75}As. The red dash line is a guiding line for temperature-dependent ^{75}K at high temperature, indicating a decreasing of ^{75}K with increasing temperature, which is also confirmed by bulk susceptibility measurement [22]. Both Knight shifts below T^* follow a same temperature-dependent behavior, which is also confirmed by the ^{133}K-^{75}K plot in the inset. (b) Temperature-dependent nuclei spin-lattice relaxation for both ^{75}As and ^{133}Cs nuclei. The blue triangles represent the nuclei spin-lattice relaxation of ^{133}Cs nuclei. The red squares represents the nuclei spin-lattice relaxation of ^{75}As. Both nuclei spin-lattice relaxation below T^* follow a same power-law behavior, which is also confirmed by the $\frac{1}{^{133}T_1}$-$\frac{1}{^{75}T_1}$ plot in the inset. The fitting formula of spin-lattice relaxation decay is $I(t) = I_0 + I_1(0.1e^{-(\frac{t}{T_1})^r} + 0.9e^{-(\frac{6t}{T_1})^r})$ for ^{75}As nuclei and $I(t) = I_0 + I_1 e^{-(\frac{t}{T_1})^r}$ for ^{133}Cs nuclei.

the contribution due to $3d_{xy}$ or $3d_{x^2+y^2}$ orbitals, the absence of the local spin behavior in temperature-dependent ^{133}K is obvious. Therefore, the local spin behavior and the incoherent-to-coherent crossover in temperature-dependent ^{75}K are ascribed to the $3d_{xy}$ or $3d_{x^2+y^2}$ orbitals. Based on previous theoretical calculation [20,26], the $3d_{x^2+y^2}$ orbital has much less mass renormalization effect than other $3d$ orbitals. Therefore, the high-temperature localized spin behavior is further constrained to $3d_{xy}$ orbital, which is consistent with the fact that the $3d_{xy}$ orbital has the maximum mass renormalization effect among all $3d$ orbitals [20,26]. In one word, we conclude that the temperature dependence of ^{133}K is dominated by itinerant $3d_{xz}$, $3d_{yz}$, and $3d_{z^2}$ orbitals, while the temperature dependence of ^{75}K at high temperature is dominated by the localized $3d_{xy}$ orbital, which is responsible for the incoherent-to-coherent crossover and local spin behavior. It should be emphasized that although the temperature dependence of high-temperature ^{75}K is dominated by the localized $3d_{xy}$ orbital, the contribution from itinerant $3d_{xz}$, $3d_{yz}$, and $3d_{z^2}$ orbitals is not negligible. Therefore, without the knowledge of the orbital-dependent hyperfine coupling tensor A_σ, it is very difficult to completely decouple the total Knight shift into separated contribution from each orbital by the present site-selective NMR measurement. However, this would not affect the qualitative conclusion in this work. The results definitely confirm the breakdown of single spin-fluid model in $CsFe_2As_2$. On the other hand, by scaling both temperature-dependent ^{75}K and ^{133}K, we found an identical temperature-dependent behavior below $T^* \sim 75$ K. As shown in the inset of Fig. 2(a), single spin-fluid behavior is valid below T^*. These results indicate that, although the single spin-fluid model is broken above T^* due to the coexistence of localized and itinerant $3d$ electrons, a coherent state involving both localized and itinerant $3d$ electrons appears below T^*, so that it follows the single spin-fluid model. Similar incoherent-to-coherent crossover behavior was observed in FeSe-derived superconductors by ARPES, in which the high-temperature incoherent state is ascribed to the so-called orbital-selective Mott phase [18,19]. In the present case, the incoherent state above T^* perhaps stems from the same orbital-selective Mott phase. Previous ARPES and STM experiments have observed a coherent peak due to below 20 K in KFe_2As_2 [27], which is due to $3d_{xy}$ orbital close to Fermi level. Further ARPES experiment in whole temperature range is needed to verify the exact nature of the high-temperature incoherent state in $CsFe_2As_2$.

In Fig. 2(b), we further measured the temperature-dependent $1/T_1$ of both ^{75}As and ^{133}Cs nuclei. In general, the spin-lattice relaxation rate $(1/T_1)$ in NMR experiment is related to the dynamical magnetic susceptibility $\mathrm{Im}\chi_\perp(q,\omega_n)$ with $\frac{1}{T_1} = 2\gamma_n^2 T \sum_q A_\perp^2(q) \frac{Im\chi_\perp(q,\omega_n)}{\omega_n}$ [28], where $A_\perp(q)$ is the hyperfine coupling tensor perpendicular to external field direction at ^{75}As or ^{133}Cs sites and $\omega_n = \gamma_n H$ is the NMR frequency. Based on symmetry analysis, in contrast to Knight shift, the off-diagonal terms in the hyperfine coupling tensor plays a key role on $1/T_1$ when $\mathrm{Im}\chi_\perp(q,\omega_n)$ mainly comes from spin fluctuation at finite q value (see Supplemental Material [23] for details). In fact, previous neutron scattering experiments have shown a significant incommensurate spin fluctuation at $[\pi(1 \pm \delta),0]$ with $\delta = 0.16$ in KFe_2As_2 [29]. Therefore, the off-diagonal terms in hyperfine coupling tensor are dominated for $1/T_1$ in $CsFe_2As_2$. Such off-diagonal term is also from the transferred hyperfine interaction (probably through overlapping between $3d$ and $4p/6p$ orbitals) [30]. Similar orbital selectivity as shown in Knight shift should be also expected for $1/T_1$. In fact, the temperature-dependent $1/T_1$ does show a distinct temperature-dependent behavior for both ^{75}As and ^{133}Cs nuclei above T^*. For ^{133}Cs nuclei, the temperature-dependent $1/T_1$ follows an approximate power-law behavior with $1/T_1 \sim T^{1.36}$, which looks like a strange metallic behavior. For ^{75}As nuclei, the temperature-dependent $1/T_1$ is almost temperature independent, which supports a localized moment behavior consistent with the Knight shift result [22]. This result further confirms the breakdown of the single spin-fluid model above T^*. Below T^*, an identical

temperature-dependent behavior for both ^{75}As and ^{133}Cs nuclei with $1/T_1 \sim T^{0.75}$ shows up as shown in the inset of Fig. 2(b). These results are consistent with the formation of coherent state below T^*. A deviation from $T^{0.75}$ power-law behavior is observed below 5 K. This is due to the appearance of a field-induced two-component behavior in spin-lattice relaxation decay, which might be related to other novel effects [22,25]. However, above 5 K, the low-temperature $T^{0.75}$ power-law behavior is ascribed to a characteristic property of the low-temperature coherent state. Next, we would like to discuss the origin for the huge difference in the value of $1/T_1$ for ^{75}As and ^{133}Cs. Since such difference in $1/T_1$ can not be scaled by corresponding Knight shift (see Supplemental Material [23] for details), how to understand the difference in the value of $1/T_1$ is not straightforward. As similar to the situation in Knight shift, only $3d_{xz}$, $3d_{yz}$, and $3d_{z^2}$ orbitals contribute to the $1/T_1$ for ^{133}Cs while the five $3d$ orbitals contribute to $1/T_1$ for ^{133}Cs nuclei. Therefore, in order to understand the huge difference in $1/T_1$, the contribution due to $3d_{xy}$ orbital in the value of $1/T_1$ must be much larger than others and the total $1/T_1$ for ^{75}As nuclei is then approximated to $1/T_1$ due to $3d_{xy}$ orbital. If we assume a comparable hyperfine coupling tensor for all $3d$ orbitals at ^{75}As sites, the above result suggests that the imaginary part of dynamic spin susceptibility $\mathrm{Im}\chi_\perp(q,\omega_n)$ should be dominated by the $3d_{xy}$ orbital. However, an orbital-dependent hyperfine coupling tensor, which is only strongly coupled to the $3d_{xy}$ orbital, could also explain our results. This needs further theoretical investigation on the details of hyperfine coupling tensor at ^{75}As site.

IV. DISCUSSION

Based on the above results on Knight shift and nuclear spin-lattice relaxation, we found that the high-temperature incoherent state above T^* conforms to the so-called orbital-selective Mott phase [15–17], in which the $3d_{xy}$ orbital is probably localized and other $3d$ orbitals remain itinerant. As shown in Fig. 3(a), the orbital-selective Mott phase has been proposed in the phase diagram based on strong coupling theory [14,16]. The theoretical study suggests that the orbital-selective Mott localization happens at the $3d_{xy}$ orbital in $A\mathrm{Fe_2As_2}$ (A = K, Rb, Cs) [20,26], which is confirmed by our present site-selective NMR results. In detail, the contrasting temperature dependence of ^{133}K and ^{75}K suggests that the orbital-selective Mott localization or at least the strongest correlation effect happens at the $3d_{xy}$ orbital, which leads to a localized spin behavior above T^*. Further ARPES experiments are needed to verify the exact nature of $3d_{xy}$ orbital above T^*.

Below T^*, a coherent state between localized and itinerant $3d$ orbitals is developed, which is also confirmed by ARPES and STM results on $\mathrm{KFe_2As_2}$ [27]. We now address the question of how to understand the underlying mechanism of such incoherent-to-coherent crossover. In fact, the incoherent-to-coherent crossover has already been proposed in early dynamical mean-field theory (DMFT) by Haule and Kotliar [31], in which each $3d$ orbital has a different crossover temperature, but the lowest one determines the crossover temperature for the whole system [32]. Recently, this scenario has been further developed by using numerical renormalization group as a viable multiband impurity solver for DMFT, suggesting that

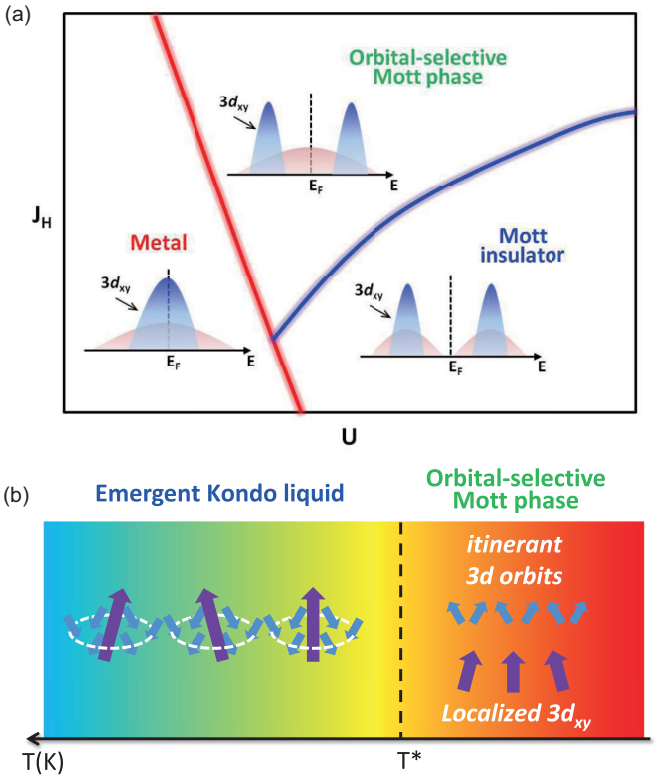

FIG. 3. (a) Schematic phase diagram of Fe-based superconductors tuned by on-site Coulomb repulsion U and Hund's coupling J_H [16,17]. When both of U and J_H are small, the system is a normal metal. When J_H is moderate but U is enough large, the system will enter into Mott insulating phase. When J_H become enough large, an orbital-selective Mott phase will replace the Mott insulating phase in the phase diagram. (b) Illustration of microscopic picture for the incoherent-to-coherent crossover. At high temperature, the system behaves as an orbital-selective Mott phase with both localized and itinerant $3d$ electrons. Below T^*, the system enters into a Kondo liquid state, in which all $3d$ electrons become coherent through Kondo-type coupling.

strong Kondo-type screening correlation exists during the incoherent-to-coherent crossover [33]. On the other hand, our previous NMR study also observed a Knight shift anomaly and relevant scaling behavior in $A\mathrm{Fe_2As_2}$ (A = K, Rb, Cs), which are ascribed to emergent Kondo lattice behavior of $3d$ electron system [22]. Based on all these facts, as shown in Fig. 3(b), we proposed that the emergent coherent state below T^* might be treated as a Kondo liquid state similar to that in a heavy fermion system with f electron [34,35].

In the f-electron heavy fermion system, the Kondo liquid state is an emergent state due to collective Kondo coupling between localized and itinerant electrons. In the Kondo liquid state, the localized spin degree of freedom is screened out by itinerant electrons, which leads to the deconfinement of localized moments. In the present case, a similar deconfinement of localized $3d$ electrons happens due to certain Kondo-type coupling between localized and itinerant $3d$ electrons, such as off-site Kondo coupling [36]. Therefore, the Kondo-type coupling between localized and itinerant spin degree of freedom for $3d$ electrons should be an important ingredient in an

effective theoretical model for Fe-based superconductors [7]. This definitely stimulates further theoretical investigation in AFe_2As_2 (A = K, Rb, Cs) system and brings new understanding on the mechanism of superconducting pairing in Fe-based superconductors.

Finally, we would like to address that the strong coupling feature observed in AFe_2As_2 (A = K, Rb, Cs) is probably due to the Mott insulating phase at $3d^5$ configuration [14,21]. Based on DMFT calculation, the realization of Mott insulating phase would be much easier at half filling than other integer fillings [17]. For example, the critical mutual Coulomb repulsion (U_c) for Mott transition has a minimum at half filling. For $3d$ electron system, the half filling is the $3d^5$ configuration. In Fe-based superconductors, the parent compound with $3d^6$ configuration is indeed a bad metal but not a Mott insulator. However, a real Mott insulating phase at $3d^5$ configuration is anticipated and this has been proposed in previous theory [21]. In this case, when we doped considerable holes in the parent compound with $3d^6$ configuration, the system is actually approaching to Mott insulating phase at $3d^5$ configuration. Therefore, the emergence of orbital-selective Mott phase between $3d^5$ configuration and $3d^6$ configuration is not surprising in strong coupling scenario. Further experimental and theoretical surveys are needed to figure out the exact nature of strongly correlated physics in this regime.

ACKNOWLEDGMENTS

This work is supported by the National Key R&D Program of the MOST of China (Grants No. 2016YFA0300201, and No. 2017YFA0303000), the National Natural Science Foundation of China (Grants No. 11522434, No. 11374281, and No. U1532145), Science Challenge Project (Grant No. TZ2016004), the Fundamental Research Funds for the Central Universities and the Chinese Academy of Sciences. T.W. acknowledges the Recruitment Program of Global Experts and the CAS Hundred Talent Program.

[1] P. A. Lee, N. Nagaosa, and X.-G. Wen, Rev. Mod. Phys. **78**, 17 (2006).
[2] F. C. Zhang and T. M. Rice, Phys. Rev. B **37**, 3759 (1988).
[3] H. Alloul, T. Ohno, and P. Mendels, Phys. Rev. Lett. **63**, 1700 (1989).
[4] M. Takigawa, A. P. Reyes, P. C. Hammel, J. D. Thompson, R. H. Heffner, Z. Fisk, and K. C. Ott, Phys. Rev. B **43**, 247 (1991).
[5] M. Yi, Y. Zhang, Z.-X. Shen, and D. H. Lu, npj Quantum Materials **2**, 57 (2017).
[6] Z. P. Yin, K. Haule, and G. Kotliar, Nat. Mater. **10**, 932 (2011).
[7] Y.-Z. You and Z.-Y. Weng, New J. Phys. **16**, 023001 (2014).
[8] H.-J. Grafe, G. Lang, F. Hammerath, D. Paar, K. Manthey, K. Koch, H. Rosner, N. J. Curro, G. Behr, J. Werner, N. Leps, R. Klingeler, H.-H. Klauss, F. J. Litterst, and B. Büchner, New J. Phys. **11**, 035002 (2009).
[9] P. J. Hirchfeld, M. M. Korshunov, and I. I. Mazin, Rep. Prog. Phys. **74**, 124508 (2011).
[10] A. V. Chubukov, Annu. Rev. Condens. Matter Phys. **3**, 57 (2012).
[11] L. Ma, G. F. Ji, J. Dai, J. B. He, D. M. Wang, G. F. Chen, B. Normand, and W. Yu, Phys. Rev. B **84**, 220505(R) (2011).
[12] K. Kitagawa, Y. Mezaki, K. Matsubayashi, Y. Uwatoko, and M. Takigawa, J. Phys. Soc. Jpn. **80**, 033705 (2011).
[13] L. Ma, J. S. Zhang, D. M. Wang, J. B. He, T. L. Xia, G. F. Chen, and W. Q. Yu, Chin. Phys. Lett. **29**, 067402 (2012).
[14] R. Yu, J.-X. Zhu, and Q. Si, Curr. Opin. Solid State Mater. Sci. **17**, 65 (2013)
[15] V. I. Anisimov, I. A. Nekrasov, D. E. Kondakov, T. M. Rice, and M. Sigrist, Eur. Phys. J. B **25**, 191 (2002).
[16] L. dé Medici, S. R. Hassan, M. Capone, and X. Dai, Phys. Rev. Lett. **102**, 126401 (2009).
[17] A. Georges, L. de Medici, and J. Mravlje, Annu. Rev. Condens. Matter Phys. **4**, 137 (2013).
[18] M. Yi, D. H. Lu, R. Yu, S. C. Riggs, J.-H. Chu, B. Lv, Z. K. Liu, M. Lu, Y.-T. Cui, M. Hashimoto, S.-K. Mo, Z. Hussain, C. W. Chu, I. R. Fisher, Q. Si, and Z.-X. Shen, Phys. Rev. Lett. **110**, 067003 (2013).
[19] M. Yi, Z. K. Liu, Y. Zhang, R. Yu, J. X. Zhu, J. J. Lee, R. G. Moore, F. T. Schmitt, W. Li, S. C. Riggs, J. H. Chu, B. Lv, J. Hu, M. Hashimoto, S. K. Mo, Z. Hussain, Z. Q. Mao, C. W. Chu, I. R. Fisher, Q. Si, Z. X. Shen, and D. H. Lu, Nat. Commun. **6**, 7777 (2015).
[20] F. Hardy, A. E. Bohmer, D. Aoki, P. Burger, T. Wolf, P. Schweiss, R. Heid, P. Adelmann, Y. X. Yao, G. Kotliar, J. Schmalian, and C. Meingast, Phys. Rev. Lett. **111**, 027002 (2013).
[21] L. dé Medici, G. Giovannetti, and M. Capone, Phys. Rev. Lett. **112**, 177001 (2014).
[22] Y. P. Wu, D. Zhao, A. F. Wang, N. Z. Wang, Z. J. Xiang, X. G. Luo, T. Wu, and X. H. Chen, Phys. Rev. Lett. **116**, 147001 (2016).
[23] See Supplemental Material at http://link.aps.org/supplemental/10.1103/PhysRevB.97.045118 for details of temperature-dependent spectra of ^{75}As and ^{133}Cs nuclei, general formula of Knight shift and spin-lattice relaxation rate for ^{75}As and ^{133}Cs nuclei, evidence for nearly isotropic Knight shift of ^{133}Cs, the relationship between Knight shift and spin-lattice relaxation rate for ^{75}As and ^{133}Cs sites.
[24] A. F. Wang, B. Y. Pan, X. G. Luo, F. Chen, Y. J. Yan, J. J. Ying, G. J. Ye, P. Cheng, X. C. Hong, S. Y. Li, and X. H. Chen, Phys. Rev. B **87**, 214509 (2013).
[25] J. Li, D. Zhao, Y. P. Wu, S. J. Li, D. W. Song, L. X. Zheng, N. Z. Wang, X. G. Luo, Z. Sun, T. Wu, and X. H. Chen, arXiv:1611.04694.
[26] S. Backes, H. O. Jeschke, and R. Valentí, Phys. Rev. B **92**, 195128 (2015).
[27] D. L. Fang, X. Shi, Z. Y. Du, P. Richard, H. Yang, X. X. Wu, P. Zhang, T. Qian, X. X. Ding, Z. Y. Wang, T. K. Kim, M. Hoesch, A. F. Wang, X. H. Chen, J. P. Hu, H. Ding, and H. H. Wen, Phys. Rev. B **92**, 144513 (2015).
[28] K. Ueda and T. Moriya, J. Phys. Soc. Jpn. **38**, 32 (1975).
[29] C. H. Lee, K. Kihou, H. Kawano-Furukawa, T. Saito, A. Iyo, H. Eisaki, H. Fukazawa, Y. Kohori, K. Suzuki, H. Usui, K. Kuroki, and K. Yamada, Phys. Rev. Lett. **106**, 067003 (2011).

[30] K. Kitagawa, N. Katayama, K. Ohgushi, M. Yoshida, and M. Takigawa, J. Phys. Soc. Jpn. **77**, 114709 (2008).
[31] K. Haule and G. Kotliar, New J. Phys. **11**, 025021 (2009).
[32] Z. P. Yin, K. Haule, and G. Kotliar, Phys. Rev. B **86**, 195141 (2012).
[33] K. M. Stadler, Z. P. Yin, J. von Delft, G. Kotliar, and A. Weichselbaum, Phys. Rev. Lett. **115**, 136401 (2015).
[34] Y.-F. Yang, Z. Fisk, H.-O. Lee, J. D. Thompson, and D. Pines, Nature (London) **454**, 611 (2008).
[35] Y.-F. Yang, and D. Pines, Proc. Natl. Acad. Sci. USA **109**, E3060 (2012).
[36] V. I. Anisimov, M. A. Korotin, M. Zolfl, T. Pruschke, K. LeHur, and T. M. Rice, Phys. Rev. Lett. **83**, 364 (1999).